

THE OFFICIAL MAGAZINE OF THE OCEANOGRAPHY SOCIETY

Oceanography

CITATION

Pinkel, R., M. Buijsman, and J.M. Klymak. 2012. Breaking topographic lee waves in a tidal channel in Luzon Strait. *Oceanography* 25(2):160–165, <http://dx.doi.org/10.5670/oceanog.2012.51>.

DOI

<http://dx.doi.org/10.5670/oceanog.2012.51>

COPYRIGHT

This article has been published in *Oceanography*, Volume 25, Number 2, a quarterly journal of The Oceanography Society. Copyright 2012 by The Oceanography Society. All rights reserved.

USAGE

Permission is granted to copy this article for use in teaching and research. Republication, systematic reproduction, or collective redistribution of any portion of this article by photocopy machine, reposting, or other means is permitted only with the approval of The Oceanography Society. Send all correspondence to: info@tos.org or The Oceanography Society, PO Box 1931, Rockville, MD 20849-1931, USA.

Breaking Topographic Lee Waves in a Tidal Channel in Luzon Strait

BY ROBERT PINKEL, MAARTEN BUIJSMAN, AND JODY M. KLYMAK

ABSTRACT. Barotropic tides generate energetic internal tides, smaller-scale waves, and turbulence as they flow through Luzon Strait, between Taiwan and the Philippines. Three-dimensional numerical simulations of this process suggest that small-scale lee waves will form and break preferentially in “outflow channels,” trough-like depressions that descend the strait’s flanks. In the simulations, these sites are the locations of the most intense dissipation in the eastern strait. To investigate this numerical prediction, an 11-day cruise on R/V *Roger Revelle* was devoted to exploring an outflow channel on the eastern slope of the strait, north of Batan Island. Using a rapidly profiling conductivity-temperature-depth sensor and shipboard Doppler sonars, observations of velocity and density fields were made at four sites in the channel. At Site III, approximately 4 km offshore the crest, the generated lee wave was found to occupy much of the water column. It expanded upward from the seafloor as an irregular disturbance with a dominant vertical scale of 250 m. Sea-surface horizontal currents exceeded 1.5 m s^{-1} and were sufficient to cause surface waves to break at 1,300 m above the local topography. Widespread internal wave breaking appeared initially at the seafloor and spread to much of the water column during the outflow phase of the tide. Breaking was also seen to a lesser extent on the inflow phase, as Pacific waters were advected westward toward the crest. The average dissipation rate at Site III, 8 W m^{-2} , exceeds typical wind energy input rates by four orders of magnitude.

INTRODUCTION

While the deep sea is generally isolated from the surface layers, localized sites of rapid vertical exchange are now being discovered. These sites are associated with either the generation or dissipation of the internal tide where topography and tides strongly interact. A number of mixing mechanisms have been identified at these sites, including both bores

and lee waves. The bores can propagate either upslope or downslope (Aucan, et al., 2006; Klymak, et al., 2011) and can extend for 200–300 m above the seafloor, producing mixing regions of comparable size. Tidal flow over topography such as ridge crests and seamounts can also produce small-scale lee waves (Legg and Klymak, 2008) with horizontal wavelengths much smaller than comparable

waves of tidal frequency.

Figure 1 presents a numerical illustration of the bore-lee wave phenomenon for the site described below. The offshore flowing currents (red, Figure 1a) separate from the slope in a series of “jumps” that extend nearly 1,000 m above the local seafloor. This pattern is maintained through the peak of the ebb tide. Isopycnal surfaces are tilted to vertical orientation and even inverted in “overtorns” that can be several hundred meters high. Modeled dissipation occurs in the overtorns, as well as in regions of large isopycnal separation (Figure 1b).

Although lee waves are thought to be widespread (e.g., Nikurashin and Ferrari, 2010), and can be modeled numerically (Klymak et al., 2010), direct observations of the phenomenon in the deep sea are rare. Their presence was inferred in observations from the Floating Instrument Platform (FLIP) in the Hawaii Ocean Mixing Experiment (Pinkel et al., 2000; Klymak et al., 2008). Recently, Nash et al. (2007), presented observations from the Oregon slope showing mid-water instabilities of the semidiurnal internal tide at depths of 2,000 m. There remains a need to observe this phenomenon with precision

sufficient to test the accuracy of contemporary numerical models.

Toward this end, we present recent data from the Office of Naval Research (ONR)-sponsored 2010–2011 Internal Waves In Straits Experiment (IWISE), where extensive measurements of tidal generation and mixing processes were made in Luzon Strait. Here, the surface tides lose over 60 GW to internal tides and local mixing (Alford et al., 2011), rendering the strait one of Earth’s most energetic tidal conversion sites. Numerous nonlinear phenomena are available for study, each associated with specific features of the strait’s topography. The challenge is to be able to sample fast enough and deep enough to resolve both the processes of interest and the larger context in which they occur.

Two-dimensional numerical models provided initial guidance for IWISE. These models focused attention on the strait’s ridge-like features and on the lee waves and bores associated with flow over ridges (recent work of author Buijsman and colleagues). With the adaptation of the three-dimensional hydrostatic MIT GCM (global circulation model) code to strait topography, a very different picture emerged. The cross-strait flows forced by the surface tides vastly prefer to flow around, not over, the ridges, following distinct channels (~ 1 km deep) as they traverse the shallow regions of the strait (Figure 2a). Classical bores and lee waves are found near the termini of these channels, as the modeled flows descend/ascend from/to the deep sea (Figures 1a,b and 3).

Given this invaluable numerical reconnaissance, experiment participants decided to spend one of the IWISE 2011 legs searching for lee waves in the region

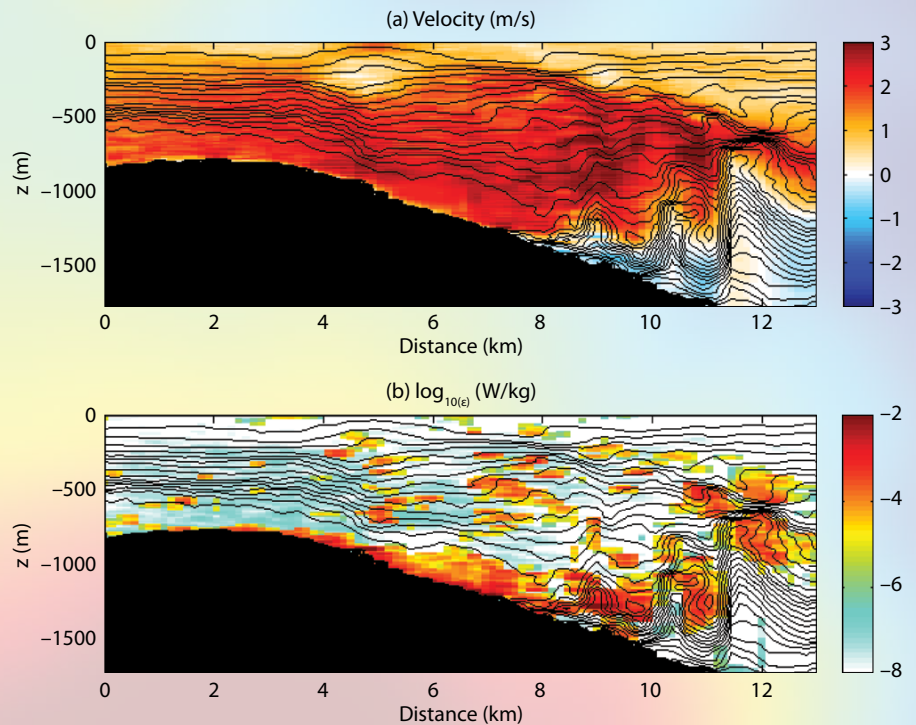


Figure 1. Along-channel section of velocity (top) and dissipation bottom from the Massachusetts Institute of Technology (MIT) three-dimensional hydrostatic numerical model showing lee wave formation as the flow descends the channel. Vertical excursions of 500 m are anticipated over comparable horizontal distances. In such a flow, variations in ship position scramble spatial and temporal variability. Enhanced dissipation (bottom) is found in the model in regions of isopycnal slope and/or dilation.

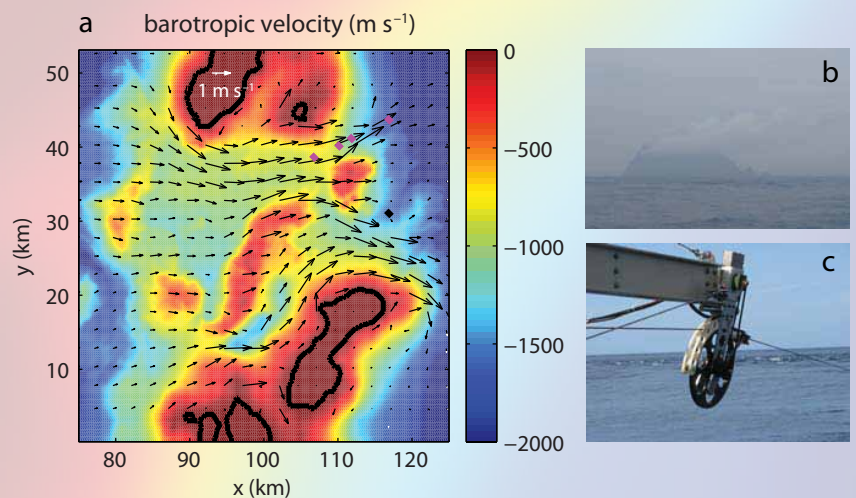


Figure 2. (a) Plan view of the Windy Island region of Luzon Strait. Barotropic current vectors from the MIT three-dimensional global circulation model are shown. Measurement stations in the north outflow channel are shown in magenta. Site III, featured in subsequent figures, is the second eastward-most site, at a water depth of ~ 1,300 m. (b) Proximity to adjacent islands and submarine topography rendered ship maneuvering challenging in the strong currents and winds. (c) The motorized sheave that tends the cable from the Fast-CTD. The standing pattern of breaking waves in the distance is a surface manifestation of the internal lee wave generated by the deep topography.

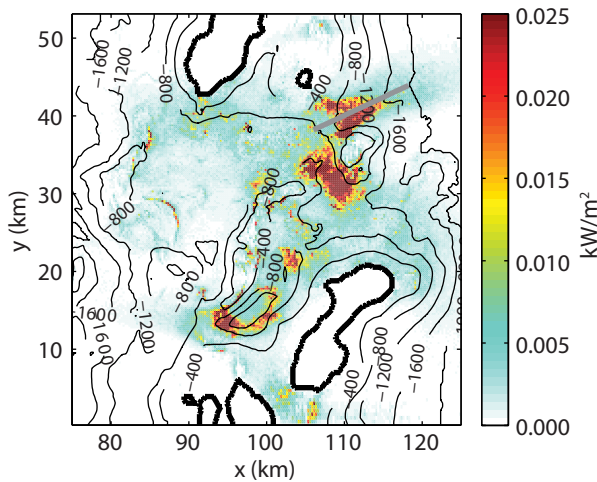


Figure 3. Plan view of the experiment site showing depth-integrated time-averaged dissipation from the MIT global circulation model. The concentration of mixing in the outflow channels, as opposed to over topographic crests, is striking. The gray line shows the location of the section in Figure 1.

between Itbayat and Batan Islands. There, the principal cross-strait pathway bifurcates into two outflow channels. Each channel appeared sufficiently two dimensional that a series of along-axis measurements might describe the flows. With the channels cresting at depths less than 1 km, it was hoped that the flows of interest would occur within the depth range of our shipboard instruments.

OBSERVATIONS

Measurements were collected on a July 11–22 leg of R/V *Roger Revelle*. Spring tides peaked on July 14, early in the measurement period. Specific objectives were to observe the evolving vertical structure in the lee waves through the tidal cycle as well as to document the mixing events and the nature of the instabilities that triggered them. Both of these studies can be compared with model predictions.

The equipment onboard R/V *Revelle* included the Hydrographic Doppler

Sonar System (HDSS), a nested set of 140 and 50 kHz sonars interfaced to the ship's positional and navigational gear in order to produce vertical profiles of absolute ocean velocity. The 140 kHz sonar profiles to depths of 300 m with 6 m depth resolution, while the 50 kHz system profiles to depths of ~1 km with 22 m depth resolution. Velocity profiles are calculated at one-minute intervals and smoothed to 10 minutes for display. The IWISE density field was sampled with the Scripps Institution of Oceanography Fast-CTD—an SBE-49 conductivity-temperature-depth instrument packaged in a streamlined drop-body and profiled vertically at speeds of 3–6 m s⁻¹. The system can profile the upper kilometer of the sea in 12 minutes (round trip), the upper 2 km in 30 minutes. With a depth resolution of ~2 m, it cannot resolve “microstructure.” However, at these intense mixing sites, energy dissipation rates can be inferred from the heights and frequencies of the

larger density overturns (Dillon, 1982), which often exceed 100 m in amplitude.

The experiment plan was to occupy a series of stations along the axis of the north outflow channel (Figure 2a), each for at least one full cycle of the diurnal tide. By obtaining depth time series at a set of fixed stations, we hoped to be able to piece together the complete space-time variability of the velocity and density fields in the channel. The effort to keep fixed stations was challenged by the strong currents in the channel coupled with winds typically exceeding 20 kts, related to a passing typhoon. Gaps occurred in the CTD time series when profiling was paused to reposition the ship. Sonar data were occasionally interrupted when rough conditions created under-hull bubbles that impeded acoustic propagation.

Analysis of the IWISE data is in a preliminary state. Here, we present observations from Site III (Figure 2a, 20°40.6'N 122°0.0'E). These data are of particular interest in that the ship was positioned directly in the lee wave as it formed over the eastward slope of the strait. The wave signal was even evident at the sea surface, in a standing band of breaking surface waves (Figure 2c) that maintained position astern of the ship for approximately three hours as both moved at ~3 kts to the west-southwest into the outflow current. As the current subsided, the waves advanced up channel, eventually passing *Revelle*. Surface manifestations of 1,000 m deep topography are not often observed.

The lee wave developed immediately with the initiation of the (eastward) offshore flow and expanded upward from the seafloor at a rate of 300–500 m hr⁻¹ as shown in Figure 4. The initially coherent

Robert Pinkel (rpinkel@ucsd.edu) is Professor, Scripps Institution of Oceanography, University of California, San Diego, La Jolla, CA, USA. **Maarten Buijsman** is Postdoctoral Research Scientist, Atmospheric and Ocean Sciences Program, Princeton University, Princeton, NJ, USA. **Jody M. Klymak** is Assistant Professor, School of Earth and Ocean Sciences, University of Victoria, Victoria, BC, Canada.

large-scale wave developed smaller-scale spatial/temporal structure with increasing altitude. This variability is marginally aliased by the relatively slow sampling (12–15 minutes per 1,200 m profile) of the F-CTD as the ship shifts position with respect to the disturbance. The long-term persistence of the surface manifestation suggests that temporal variability is slow in the frame of the wave. The high-frequency motions subside quickly with cessation of offshore flow. The “remnant lee wave” is then advected back into the strait where it later appears at our shallower measurement stations. Note that surface and internal tidal currents combine such that the eastward outflow from the South China Sea into the Pacific occupies only ~ 25% of the diurnal tidal cycle. The “relaxed” inflow occurs at speeds approaching 0.5 m s^{-1} , with vertical isopycnal displacements of 100 m.

To document the incidence of

turbulent overturning of the fluid, we first smooth density profiles by 20 m in the vertical and determine the incidence of negative density gradients. Such regions are plotted as dark dots against background fields of horizontal kinetic energy (HKE), log shear squared (S^2), and log strain in Figure 5. Note that the periods of high HKE (Figure 5a) are highly concentrated. In the July 13 outflow event, breaking rates peak following cessation of the strong currents. This pattern is seen consistently in the upper ocean, where overturns are found primarily in low-HKE regions. The waves that presumably cause this overturning have very little HKE relative to the fundamental tide.

Principal deep-breaking events occur at Site III during periods of low shear (Figure 5b, days 13.2–13.5, 14.2–14.4, and 15.3–15.5, below 500 m.). The dominant lee waves are of sufficiently large

scale that the low ambient shears are not significantly increased.

In the upper ocean, ambient shear is robust and there is some evidence of enhanced breaking in high-shear regions. Principal examples are found during periods of slack tide or tidal (westward) inflow in the aftermath of the lee-wave episodes.

Strain (Figure 5c) is here defined as the instantaneous separation of a pair of isopycnal surfaces divided by their time-mean separation. Density profiles are first Thorpe-sorted (Thorpe, 1977) prior to calculation of isopycnal depths. When large-scale overturning is prevalent, strain estimates are sensitive to the sorting process. Space-time aliasing also makes for apparently rapid strain variations, although they are largely obscured by the markers indicating overturning events. In the upper 300 m and at all depths during periods of on-ridge

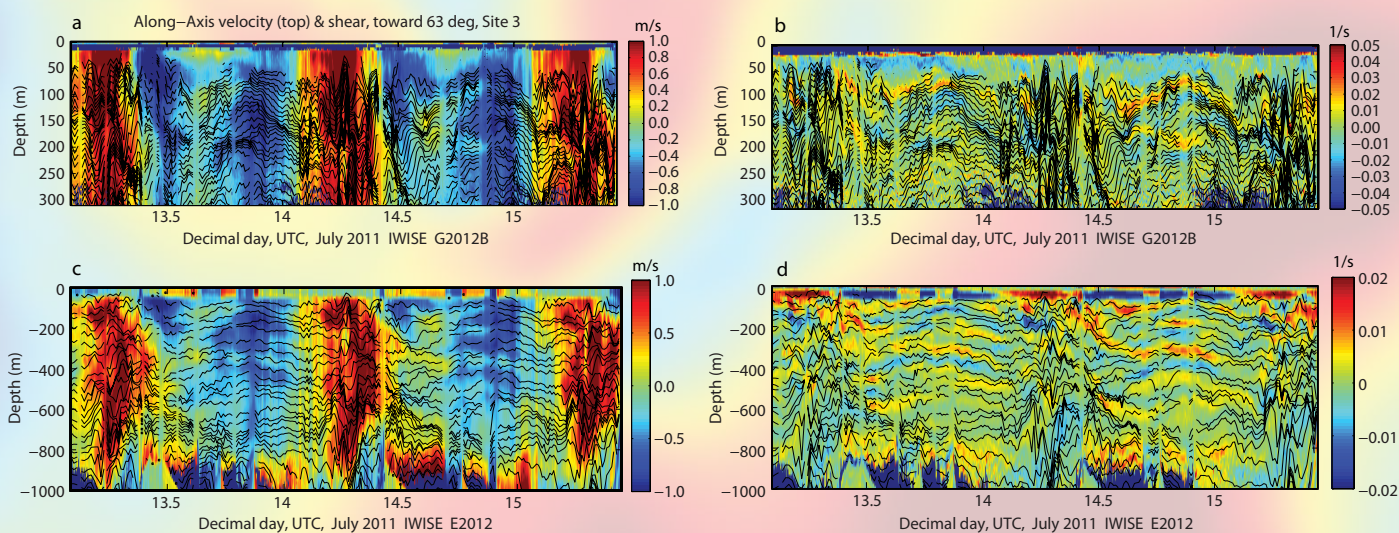


Figure 4. A 2.5 day record of along-axis current (positive toward 63° , a, c) and shear (b, d) from the HDSS 140 kHz sonar (a, b) and 50 kHz sonar (c, d) on R/V *Revelle*. Isopycnals, separated in the mean by 10 m (top) and 40 m (bottom), are overplotted. Outflow periods are characterized by rapid vertical motion of the isopycnals, with ~ 200 m vertical coherence scales at depth, diminishing in the upper ocean. Low-frequency motions that are highly coherent in the vertical dominate inflow periods. The dominant shears are not clearly associated with tidal phenomena, although shear layers are advected vertically with tidal motions. Cross-channel shear (not shown) is comparable in magnitude and vertical scale to along-channel shear.

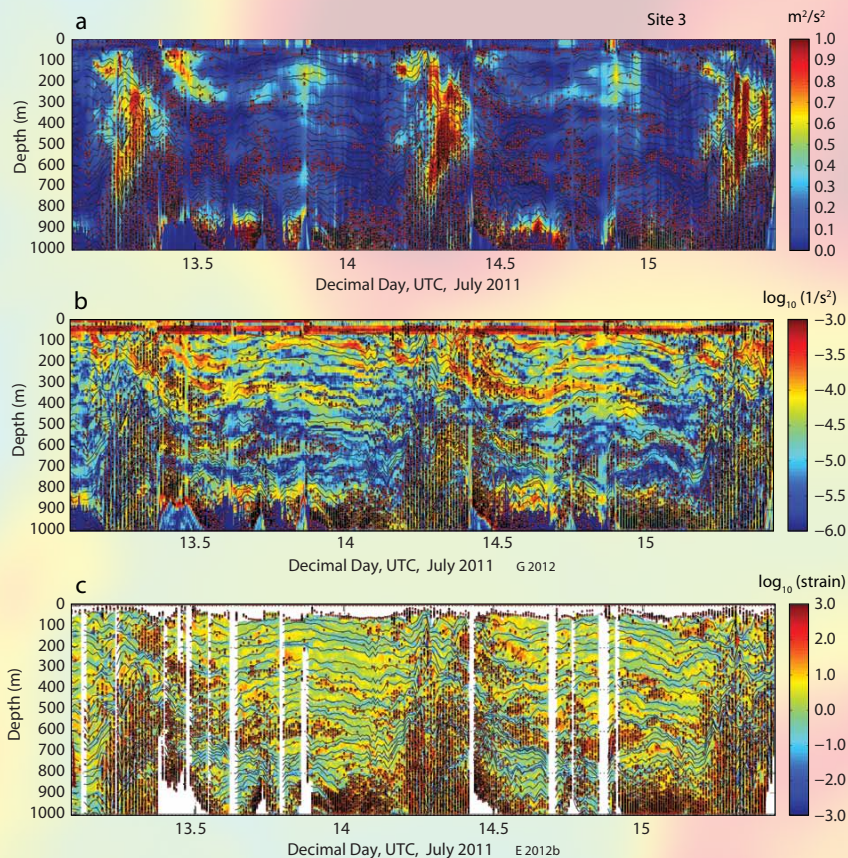


Figure 5. (a) Maps of horizontal kinetic energy, (b) $\log_{10}(\text{shear squared})$, and (c) $\log_{10}(\text{strain})$ for the Site III record. The presence of overturns of vertical scale 20 m or larger is indicated by dots. See text for discussion.

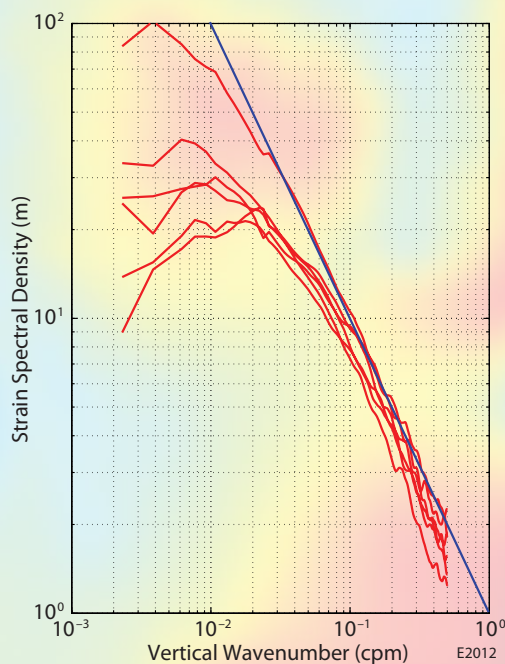


Figure 6. Vertical wavenumber spectra of strain, $S(k)$, obtained over the depth range 100–800 m and averaged into successive four-hour estimates over the 24-hour tidal cycle. The strain spectrum is at maximum when lee waves are present. Spectra are nominally estimated at 64 degrees of freedom in the lowest wavenumber bands. Additional smoothing is employed to increase statistical stability with increasing wavenumber. The reference $S(k) = k^{-1}$ is drawn.

flow, overturning is found principally in regions of large positive strain/reduced buoyancy frequency, consistent with previous open-ocean observations (Alford and Pinkel, 2000).

Klymak et al. (2010) suggest that the dominant vertical scale of the growing lee waves is related to the horizontal speed of the barotropic tidal flow. Lee wave horizontal phase speed, which is proportional to vertical scale, must then be sufficiently large to allow the wave to propagate against the tidal flow in order to maintain wave position relative to the topography. This hypothesis can be investigated through estimates of the vertical wavenumber spectrum of strain, taken at various stages of the tidal cycle. In Figure 6, four-hour averages of the vertical wavenumber spectrum of strain are plotted for six intervals throughout the tidal cycle. The spectra coalesce to a somewhat common k^{-1} form at wavenumbers above 0.1 cpm. During the low-strain (return flow) periods of the tidal cycle, the strain spectrum peaks at 50–100 m vertical scale. During the lee wave events, variance density grows by a factor of five, and the dominant vertical scales increase to ~ 250 m. These scales correspond to a horizontal phase speed of order $c \sim Nk^{-1} \sim 0.25 \text{ m s}^{-1}$, significantly less than the peak speeds observed. However, the numerical simulations (Figure 1a, distance 12 km) also show ~ 250 m vertical-scale lee waves at mid-depths, overlying much larger vertical scale motions below.

Estimates of the turbulent dissipation rate of kinetic energy can be derived from the Thorpe scales of the sorted density profiles (Figure 7; Dillon, 1982). Temporally, the depth-averaged dissipation varies by a factor of 30–100

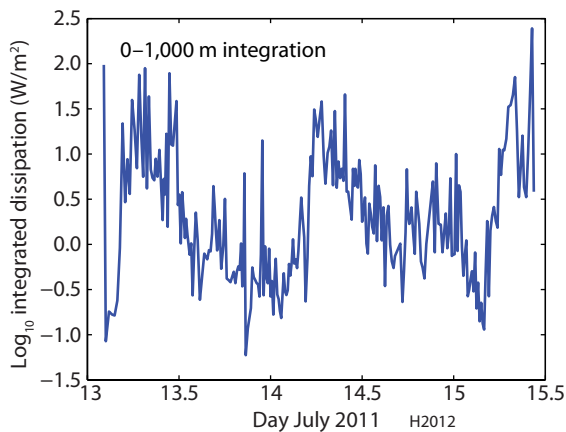


Figure 7. Site III turbulent dissipation rate integrated over the upper kilometer.

over the course of the lee wave development cycle. The time-averaged, depth-integrated dissipation is 8 W m^{-2} , in good agreement with the numerical prediction (Figure 3).

SUMMARY

Observations of internal lee wave formation were made at four stations along an outflow channel on the eastern flank of Luzon Strait. Bursts of high-frequency, long-vertical-wavelength motion emerged shortly after the onset of down-channel flow. At observation Site III, approximately 4 km downstream from the channel entry, surface current convergences associated with these internal waves are sufficient to cause ambient surface waves to break. At this site, widespread overturning is seen in the lower 600 m of the water column, starting near the seafloor roughly one to two hours after initiation of the lee-wave packet, and expanding upward. Overturning (at 20 m vertical scales and larger) quickly becomes so widespread that it is difficult to further track the vertical motion of isopycnals. Patches of overturning water are seen throughout the tidal cycle, even during the inflow period. A better picture of the spatial pattern of dissipation will form as all

measurement sites are examined.

Even with the analysis in a preliminary state, it is clear that the numerical predictions are substantially correct. Presumably, these outflow channels duct lower-frequency flows as well as the tidal flows described here. The large-scale consequences of concentrating massive tidal mixing at these flow chokepoints deserve further study.

ACKNOWLEDGEMENTS

The authors thank Mike Goldin, Tony Aja, Mai Bui, and Tyler Huguen for creation and operation of the instruments used. The captain and crew of R/V *Revelle* handled the vessel with great skill during the strong currents and crosswinds that characterized much of the experiment. This work was funded by the Office of Naval Research. 

REFERENCES

- Alford, M.H., and R. Pinkel. 2000. Observations of overturning in the thermocline: The context of ocean mixing. *Journal of Physical Oceanography* 30:805–832, [http://dx.doi.org/10.1175/1520-0485\(2000\)030<0805:OOOITT>2.0.CO;2](http://dx.doi.org/10.1175/1520-0485(2000)030<0805:OOOITT>2.0.CO;2).
- Alford, M.H., J.A. MacKinnon, J.D. Nash, H. Simmons, A. Pickering, J.M. Klymak, R. Pinkel, O. Sun, L. Rainville, R. Musgrave, and others. 2011. Energy flux and dissipation in Luzon Strait: A tale of two ridges. *Journal of Physical Oceanography* 41:2,211–2,222, <http://dx.doi.org/10.1175/JPO-D-11-073.1>.

- Aucan, J., M.A. Merrifield, D.S. Luther, and P. Flament. 2006. Tidal mixing events on the deep flanks of Kaena Ridge, Hawaii. *Journal of Physical Oceanography* 36:1,202–1,219, <http://dx.doi.org/10.1175/JPO2888.1>.
- Dillon, T.M. 1982. Vertical overturns: A comparison of Thorpe and Ozmidov scales. *Journal of Geophysical Research* 87:9,601–9,613, <http://dx.doi.org/10.1029/JC087iC12p09601>.
- Klymak, J.M., M.H. Alford, R. Pinkel, R.C. Lien, Y.J. Yang, and T.Y. Tang. 2011. The breaking and scattering of the internal tide on a continental slope. *Journal of Physical Oceanography* 41:926–945, <http://dx.doi.org/10.1175/2010JPO4500.1>.
- Klymak, J.M., R. Pinkel, and L. Rainville. 2008. Direct breaking of the internal tide near topography: Kaena Ridge, Hawaii. *Journal of Physical Oceanography* 38:380–399, <http://dx.doi.org/10.1175/2007JPO3728.1>.
- Klymak, J.M., S. Legg, and R. Pinkel. 2010. A simple parameterization of turbulent tidal mixing near supercritical topography. *Journal of Physical Oceanography* 40:2,059–2,074, <http://dx.doi.org/10.1175/2010JPO4396.1>.
- Legg, S., and J.M. Klymak. 2008. Internal hydraulic jumps and overturning generated by tidal flow over a tall steep ridge. *Journal of Physical Oceanography* 38:1,949–1,964, <http://dx.doi.org/10.1175/2008JPO3777.1>.
- Nash, J., M.H. Alford, E. Kunze, K. Martini, and S. Kelly. 2007. Hotspots of deep ocean mixing on the Oregon continental slope. *Geophysical Research Letters* 34, L01605, <http://dx.doi.org/10.1029/2006GL028170>.
- Nikurashin, M., and R. Ferrari. 2010. Radiation and dissipation of internal waves generated by geostrophic motions impinging on small-scale topography: Application to the Southern Ocean. *Journal of Physical Oceanography* 40:2,025–2,042, <http://dx.doi.org/10.1175/2010JPO4315.1>.
- Pinkel, R., W. Munk, P. Worcester, B.D. Comuelle, D. Rudnick, J. Shearman, J.H. Filloux, B.D. Dushaw, B.M. Howe, T.B. Sanford, and others. 2000. Ocean mixing studies near the Hawaiian Ridge. *Eos, Transactions American Geophysical Union* 81(46):545, <http://dx.doi.org/10.1029/EO081i046p00545-02>.
- Thorpe, S.A. 1977. Turbulence and mixing in a Scottish loch. *Philosophical Transactions of the Royal Society of London A* 28:125–181, <http://dx.doi.org/10.1098/rsta.1977.0112>.